Holographic Noise in Interferometers

Craig J. Hogan
University of Chicago and Fermilab

General arguments show that holographic theories with a maximum frequency at the Planck scale predict indeterminacy of relative transverse position in spacetime, corresponding to the diffraction limit of Planck wavelength radiation. Suitably designed instruments should display a new phenomenon, a randomly varying shear in relative position, with a flat power spectral density at low frequencies given approximately by the Planck time, and with no other parameters. An effective theory is presented to connect fundamental theory with macroscopic phenomena, such as the statistical properties of noise in signals of interferometers. A controlled theory of transverse spacetime wavefunctions is outlined, based on the paraxial wave equation with a carrier wave at the Planck frequency, and its gaussian-beam solutions. Formulas are derived in the time and frequency domain for autocorrelation of beamsplitter position. The cross-correlation between two non-coincident interferometers as a function of separation is estimated. The cross-correlation signature may be exploited in the design of experiments to provide convincing evidence for or against the holographic hypothesis.

INTRODUCTION

In quantum mechanics, a particle of energy E has a frequency $\nu = \omega/2\pi$ given by Einstein's photoelectric formula $E = h\nu = \hbar\omega$. By contrast, in General Relativity a given quantity of mass-energy is associated with a minimum length, the Schwarzschild radius $R_S = 2GE/c^4$ of a black hole, which sets a maximum frequency. These criteria collide at the Planck scale (conventionally defined as $\lambda_P/c \equiv t_P \equiv \sqrt{\hbar G_N/c^5} = 5.4 \times 10^{-44}$ seconds), setting a minimum time interval or wavelength, or maximum frequency, where quantum mechanics can be consistently described using particles and fields on a classical spacetime background.

A consistent theory of quantum spacetime cannot be achieved simply by imposing a frequency cutoff, such as filtering at the Planck frequency in some classical lab frame. A Planck length ruler in some lab frame will, in some other lab frame boosted along its length, appear shorter, violating the minimum-length restriction. The reconciliation must be achieved by a new theory that includes new, unfamiliar transformation properties.

One possible new property, again motivated by black hole physics, is holography[1–3]. In holographic theories, the world is encoded on two dimensional null sheets with one degree of freedom per 4 Planck areas, corresponding to the entropy of the null surface representing a black hole event horizon. Although there are candidates[4] for holographic theories of everything, it is not generally agreed how they map onto a system resembling a nearly-flat, macroscopic, classical spacetime. This paper presents a particular hypothesis about the classical limit of holographic theories, and about phenomenological consequences of holography in the lab, particularly in interferometers.

The Planck scale in the energy domain lies far beyond the reach of current experimental techniques. This paper argues however that in some theories, it may be possible to study Planck scale phenomena in the spacetime domain, using precise measurements of position that are coherent over macroscopic distances. Current technology using laser interferometry may be capable of detecting this new, Planck-scale physics. This works because the relative position wavefunctions of optical elements in interferometers are measured with extreme position over macroscopic distances. The positions of optical elements normal to their surfaces are measured to a precision such that the average null wavefront, across the measured transverse position error, curves by of the order of a Planck length. Thus if normal wavefunctions have a spatial frequency cutoff at the Planck length, and relative transverse positions at each longitudinal separation are holographically encoded on Planck scale light sheets, the transverse position wavefunctions have a measurable width.

Suppose there is a maximum spatial frequency at the Planck scale in any frame. That means that the spatial wavefunction of a macroscopic body does not contain physical components at higher spatial wavenumbers. The wavefunction of position in a particular dimension, say z, can be expressed as a sum of modes with a cutoff at this scale. If this were the ordinary wavefunction, it would correspond to a limit on the physical momentum of bodies at the Planck scale, which is not physical. In holographic theories, there is instead a physical limit on the mass per area, of about a Planck mass per Planck area. We suppose that this frequency-limited wavefunction is a new kind of wavefunction, that of the spacetime itself, or more precisely, that of the position of bodies within the spacetime.

At macroscopic separation along the measured z direction, relative positions of bodies are defined by a wavefunction with a Planck frequency cutoff. Measurements of their position with null particles can be made with Planck precision. However, once the z direction is chosen as the holographic frame, the relative position wavefunctions in the transverse x and y directions, at macroscopic z separation, are much less well defined. At a separation L in the z direction, the

transverse uncertainty is of order $\sqrt{\lambda_P L}$. This "holographic uncertainty" in spacetime is much larger than the Planck length.

An effective theory of this uncertainty is presented here, based on the paraxial wave equation. The macroscopic position of mass-energy in some chosen frame is described as a wavefunction. Once a lab frame and a holographic wavefront frame are chosen, the wavefunction is represented by a complex phasor relative to a carrier wave at the Planck frequency. The wavefronts of the carrier define a holographic or wavefront frame, determined by measurements. It is then possible to define eigenstates and solutions defining relative positions within this system. The effective theory describes positions in an emergent spacetime with a limiting frequency. The holographic uncertainty is precisely characterized by the transverse correlations in the wave theory, exactly like those described as diffraction in wave optics.

A potentially observable new phenomenon associated with these ideas is a universal "holographic noise": random fluctuations in the relative transverse spacetime positions of bodies widely separated in spacetime, caused in holographic theories by the indeterminacy of Planck-scale waves from which classical spacetime emerges.[5, 6] The paraxial-wave theory is used here to make well controlled statistical predictions for the effective positions of optical elements and for the time series of interferometer signals. In addition, signals in two nearby interferometers with no physical connection are highly correlated, a distinctive signature for designing an apparatus to provide convincing evidence for or against the effect.

The effect discussed here is fundamentally different from previously conjectured fluctuations of a quantum-gravitational origin (e.g., [7–9]). At the most basic level, those analyses are based on various hypotheses about quantum perturbations of a metric. Holographic noise is not due to perturbations of a metric, but to a new, in-common motion of mass-energy relative to a classical metric. In this sense holographic indeterminacy is not "quantum gravity" because it emerges only insofar as positions are defined by measurements of massive bodies. The same comment applies to purely metric fluctuations derived from noncommutative geometry: the holographic effect addresses not a space on its own, but the positions of mass-energy within the spacetime. Holographic indeterminacy and noise is precisely characterized in its spectrum and has an absolutely calibrated normalization from black hole physics. It also exhibits a new, distinctive spatial shear structure; theories based on metric perturbations correspond to strain motions, like gravitational waves. These shear modes are not physically described by metric perturbations, but by new effective motions of mass-energy within a fixed metric.

HOLOGRAPHIC INDETERMINACY

Classical spacetime is described as a continuous manifold of events. This is an approximation to reality. A real spacetime cannot be observed directly but only by measurements of mass-energy within it. Particles and bodies are assigned classical positions, and fields are described as functions of classical coordinates, but these coordinates should not be regarded as physically real except insofar as they are measured.

In quantum mechanics relative positions are ill defined because of Heisenberg uncertainty; a quantum state is described by a position wavefunction, the amplitude for a body to be measured at each position. This uncertainty can be minimized if positions are measured using massive bodies. In the analysis herein, the Heisenberg uncertainty is neglected; in other words, the ordinary wavefunction of bodies is assumed to be narrower than the Planck length.

However, there is an additional indeterminacy attached to relative positions if there is a maximum frequency or minimum fundamental time. In this case, it is unphysical to describe a position wavefunction as a function of a classical position variable. Instead, a wavefunction for a position observable, or more precisely the amplitude for observing a particular relationship of relative position between bodies, must take account of the frequency limit on their wavefunctions in some observation frame. This ambiguity is best described as a wavefunction for the spacetime itself since it occurs for any possible measurement of relative spatial position. In this view, nearly the same spacetime wavefunction applies to any bodies sharing nearly the same spacetime and the same observation frame.

Holographic indeterminacy is a particular hypothesis about how this works phenomenologically. The observation frame includes a choice of direction, and is expressed by writing a spacetime wavefunction relative to a Planck-frequency plane carrier wave representing that frame. We begin with general descriptions of the effect and its motivation, and follow with a more formal effective phenomenological theory.

Quantum Description of the Effect

Consider measurements of the positions of massive bodies at rest in a flat spacetime with a Euclidean coordinate system in some laboratory frame. The x position of body 1 is measured at time t_1 relative to some distant reference. This measurement places the position of other bodies into a definite quantum state described by a spacetime wavefunction that depends on their positions but not on their other properties. The effect of the measurement propagates at velocity c from the measurement event. If a position of body 2 is measured on this light cone, the positions of bodies 1 and 2, separated by a distance L_{12} in the yz plane, are conjugate operators, related by

$$[x_1, x_2] = -i\lambda_P L_{12}. \tag{1}$$

The width of the wavefunction describing their relative position increases with separation like $\Delta x_1 \Delta x_2 = \lambda_P L_{12}$.

This new form of indeterminacy can be described using wave mechanics of position relative to a Planck wavelength carrier wave in the lab frame. A spatial localization of a body by a measurement creates a momentum uncertainty in the same direction. In the transverse directions, this creates perturbations in the orientation of carrier wavefronts that propagate to create an uncertainty at large distances. The nonlocal propagation of the effect can be described using diffraction theory, described below.

The measurement that collapses the wavefunction can in principle be environmental. An apparatus does not itself have to make both measurements 1 and 2; as long as interactions on the past light cone of event 2 collapse transverse position states, a random "motion" — not an ordinary motion, but a change of relative position that depends on a choice of frame— can be measured between positions of massive bodies in just one direction, as measured by null particles moving along that direction. In this interpretation, although nonlocal measurements of relative position are needed to detect the effect, they could in principle be detected along one axis. The character of the resulting effective motion is that of a shear: matter (but not light) along any given line moves together, relative to that along other parallel lines, by an amount corresponding to a random walk of about a Planck length per Planck time, or transverse Planck separation. The calculation of interferometer response below is based on such a semiclassical model.

Semiclassical Description of the Effect

If the wavefunction of the macroscopic spacetime states is "collapsed" by environment on a continuing basis, the effect can be described semiclassically, as a shear motion undergoing a random walk. Although it describes a real and observable change in position, the "motion" is not ordinary classical motion, and the randomness is fundamentally quantum in nature.

In a holographic flat spacetime, the world is encoded, at Planck resolution, on a single 2D reference plane that appears, in any lab frame, to be moving at the speed of light. The transverse position of mass in another parallel plane at distance $L = ct$, relative to mass in the reference plane, is described by a wavefunction with a standard deviation $\approx \sqrt{L\lambda_P}$, the Rayleigh diffraction scale for Planck wavelength waves at distance L. The choice of a reference plane by a measurement collapses the system into an eigenstate, which we call a holographic frame. If a measurement extends over a macroscopic distance L, there is an inherent indeterminacy in relative transverse positions of order $\approx \sqrt{L\lambda_P}$.

By the same token, if the wavefunction collapses on a continuous basis, it implies that in a particular lab frame, there is a random variation of position with time. The separation of bodies separated by a distance L, as measured by null propagating photons along their separation, varies over time, like a bounded random walk, of a Planck length per Planck time. This spreading saturates however: at times separated by more than L/c, the relative measured position of the two bodies "at rest" is drawn from a distribution around a fixed classical separation, with a width $\sqrt{L\lambda_P}$. Nearby bodies, separated by much less than L, experience nearly the same apparent relative motion.

Consider events in a flat spacetime with a Euclidean coordinate system in some laboratory frame. Observer X sets up two pointlike bodies with separation L along the x axis. This is done by timing pulses of reflected radiation from a body at the origin, which we call the beamsplitter, to an end body. Observer Y sends a pulse from the beamsplitter along the y axis to an end body at the same distance L. The bodies are massive enough that we can neglect standard Heisenberg quantum uncertainty in their position. Classically, the system can be prepared in this way with everything at rest in the lab frame. With holographic indeterminacy, if pulses are sent out at the same time along the two axes, they do not return at the same time.

Consider the X frame. Photons always move at exactly c in the lab frame. At the moment $t = L/c$ when the pulse reaches the body at $x = L, y = 0$, the pulse along the y axis is at $y = L, x = 0$ in the laboratory coordinates. However, in this frame the bodies along the y axis— both the beamsplitter and the end mass— are not at their

classical positions, because they are in a plane a distance L from the reference plane. They are both displaced by the same amount, $\Delta y \approx \sqrt{L\lambda_P}$. This is described quantum-mechanically, using a wavefunction of transverse position for the center of mass of this plane. In effect all massive bodies in this plane (or any other plane normal to x) "move" together as a rigid body. At time $2L/c$, the x pulse returns to the beamsplitter: $x = y = 0, t = 2L/c$. However, the return y pulse reaches the beamsplitter at a different time. It reaches $x = y = 0$ at the time $t = 2(L + \Delta y)/c$. The same description applies in the Y holographic frame, with X and Y labels reversed. Each time this measurement is performed, Δy and Δx are both different, drawn from a distribution of standard deviation $\approx \sqrt{L\lambda_P}$. Although we have chosen $x = y = 0$ as a reference point for the beamsplitter position, the effect on arrival times is the same as holding the end bodies fixed in the lab frame and having a random motion of the beamsplitter. The effect could also be observed by comparing just a single arm with a precise clock.

The "movement" is both rigid and transverse, so it does not create differential motions of adjacent bodies measured in the same direction. Indeed it is clear that it is not an ordinary movement at all. Unlike the interaction with gravitational waves, no energy is exchanged between the spacetime and the photons.

A Michelson interferometer implements this thought-experiment by interfering light from two orthogonal paths. A wavefront interacts with the beamsplitter twice, first reflecting along one arm and then, a time $2L/c$ later, from the other. Between these reflections the beamsplitter "moves" as just described. The phase of the interference signal on short timescales behaves as if the beamsplitter, but not the other optical elements, randomly moves by about a Planck length per Planck time. For time intervals longer than $2L/c$ the apparent random motion is bounded, the width of the distribution given by $\approx \sqrt{L\lambda_P}$.

This description is helpful to understand the effect on interferometers of different layouts. For example, in unequal arm interferometers, the noise is determined by the shorter of the two arms. For an interferometer with a the second arm bent by 90 degrees to be parallel with the first, holographic noise in the arm length difference appears because of the shear motion, even if it would not appear for a gravitational wave strain; by the same token, if it is bent by 180 degrees, dark port response is sensitive to strain but not to holographic shear. Interferometers optimized to detect gravitational waves, which often have either folded arms or resonant cavities to amplify strain response, are therefore often not optimized to detect holographic shear noise. For more than one interferometer, elements sharing the same null wavefront share the same holographic displacement, even if they have no physical connection. As discussed below, these features are important in designing a system to show this effect and exclude other sources of noise.

General Arguments for Holographic Uncertainty

Nonlocal measurements of the relative transverse position of macroscopic bodies are motivated on more general grounds than just the effective wave theory presented here. The following arguments motivate experimental efforts to provide more convincing evidence for or against the holographic hypothesis.

Holographic Uncertainty from Counting Position Eigenstates

Holographic noise can be regarded as a sampling noise due to the Planck frequency limit of spacetime, or as the consequence of measuring conjugate observables (in this case, positions in different directions), in a system described by specific, finite number of degrees of freedom. In holographic theories, a bound on the number of degrees of freedom leads to a limit on the number of independent measurable transverse relative positions of macroscopic bodies in an extended system.The signal of an interferometer that compares two transverse positions displays noise as a direct consequence of the frequency bound of the fundamental theory. Conversely, a lack of quantum noise in position observables at a certain level would imply a lower bound on the number of degrees of freedom.

Consider a fundamental theory with these features:

1. *Frequency bound.* In any laboratory frame, there is a maximum frequency $c/\lambda \equiv \omega/2\pi$.

2. *Holographic information bound.* On any light sheet, there is a minimum wavelength λ in the transverse directions.

These features are related properties in holographic theories built on light sheets. In a lab frame, we can think of c/λ as the frequency of a carrier wave. In a holographic theory, this does not result in a simultaneous resolution of λ in all three dimensions everywhere at once; rather, this resolution is achieved within a 2D light sheet, which determines the holographic frame, only at single longitudinal position, and in the normal direction to it. When λ is identified with the Planck scale, such a theory approximately satisfies by construction holographic entropy bounds derived from

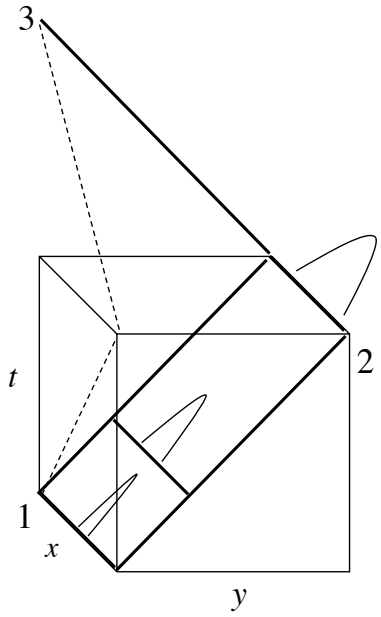

FIG. 1: Holographic spacetime, with z dimension suppressed. An x segment of a null sheet normal to y is shown, generating the emergent y dimension. The growth of transverse uncertainty is shown schematically. The dashed line shows another null trajectory, normal to x, as in the orthogonal arm of a Michelson interferometer.

black hole physics. Put another way, these features would be expected in any theory where the thermodynamical properties (such as entropy) of a black hole event horizon arises out of statistical mechanics, from quantum-mechanical degrees of freedom of spacetime.

Consider the situation illustrated in the spacetime diagram, Figure (1). This shows two dimensions of space and one of time in a lab frame; the z spatial dimension is suppressed. The inclined plane shows a segment of the x axis moving along a null trajectory, corresponding to the light sheet frame with wavefronts normal to y. In this frame, all events in this sheet occur at one time; that is, properties of the system at all x, y on this sheet are encoded holographically by the theory by data along x at $y = 0, t = 0$. Quantum relationships in this system between events at large y separation are encoded in this holographic frame by transverse correlations along x.

The most direct way to derive the uncertainty is simply to count position degrees of freedom. In the standard classical interpretation of quantum mechanics, the number of position configurations cannot exceed the number of states of the system, which means that the number of different position eigenstates for a particular body cannot exceed the number of degrees of freedom of the system. A position state can be expressed as a linear combination of a finite number of such eigenstates.

The Shannon sampling theorem tells us that two numbers per λ suffice to describe any function with no frequencies above c/λ; thus, along the transverse dimension x there is a maximum of two position eigenstates per λ. Consider positions in the x, y plane, without regard to their z position. The number of position eigenstates in the 2D x, y plane cannot exceed the information bound in the one x dimension that sweeps it out: $N < 2L_x/\lambda$, where L_x is the length of the x segment. But that number of eigenstates now has to suffice to describe positions in a two-dimensional system, the null x, y sheet.

Now suppose that an apparatus of size $L = L_y = L_x$ measures the relative positions of bodies in the x, y plane in the lab frame. For example, a Michelson interferometer with x and y arms as shown in figure (1) compares transverse wavefunctions in two different null frames, by combining light at event 3 from the two arms. Suppose that the number of position eigenstates in the x, y plane corresponds to mean separation Δx in each direction. The number of position eigenstates is $L^2/\Delta x^2 = N = 2L/\lambda$, so $\Delta x^2 = \lambda L/2$. A time series of such measurements wanders over time L/c by an amount $\approx \Delta x$, yielding a power spectral density for position, $\Phi \approx \Delta x^2 L/c \approx L^2\lambda/2c$; the dimensionless shear $\Delta L/L$ has a power spectral density given by the fundamental time, $\approx \lambda/c$. This result approximately reproduces holographic uncertainty and noise derived in other ways.

The number of position eigenstates of an interferometer with holographic indeterminacy and noise approximately saturates the holographic bound on degrees of freedom, as derived from black hole physics, if $\lambda \approx ct_P$. If holographic noise is not present in a Michelson interferometer, it implies that the system has more eigenstates for positions of its

optical elements than those bounds allow, and will rule out this class of theories.

Direct Derivation from Black Hole Entropy and Evaporation

Holographic uncertainty can also be derived directly from the requirement that black hole evaporation obeys quantum mechanical unitarity. Here we only sketch the argument without numerical factors, although it should be possible to calibrate the predicted uncertainty with a more careful calculation along these lines. Once again, we count position eigenstates, this time of locations (or directions) of particles evaporated from a black hole.

Consider a black hole of radius R_S. Very far away we have a giant spherical shell of photographic film of radius L, that completely surrounds a volume with the hole at the center. After a very long time, the hole has evaporated. Each evaporated particle has left an image on the film. In principle the arrival times can be recorded so different arrival times correspond to different states. There are about $N = (R_S/\lambda_P)^2$ particles altogether.

The number of states of the evaporated particles cannot be more than the number of states of the hole. We shall show that this is works out about right if the distant, flat spacetime has holographic uncertainty in transverse position independently of the properties of the hole.

We can think of the hole as covered in Planck size pixels. In thermal evaporation, every time $\approx R_S/c$, the hole is reduced by the typical thermal particle mass $\approx \hbar/R_S c$ and shrinks by one Planck area. The number of different ways to disassemble the hole is the number of ways this can happen N times over. It equals the number of evaporated states if for each particle the number of final directional eigenstates is also N. (Every time R_S/c there are N choices of direction. This happens N times before the hole is gone so there are $N^N = \exp N \log N$ states. The entropy is then $N \log N$. If the difference in ordering is ignored, the entropy is just $\approx N$. The ordering factor cancels in the comparison of the hole with the distant film.) Every evaporation time R_S/c there are N choices of direction, and this has to match the number of options for the image location for that particle in the final image.

Suppose there is an uncertainty Δx in the transverse positions of the particle images, so that the information, or number of degrees of freedom in the film image is $(L/\Delta x)^2$. The number of evaporated particle states matches the number of black hole states if $(L/\Delta x)^2 \approx (R_S/\lambda_P)^2$. There is no contradiction with the black hole entropy as long as

$$\Delta x^2 > L^2 \lambda_P^2 / R_S^2. \tag{2}$$

If Δx^2 were smaller than this, then the amount of information per evaporated particle would be larger than that available in the hole. It would take more data to specify the final state than is available in the initial state.

Now in addition, the ordinary Heisenberg uncertainty tells us that for the particles of energy $\hbar c/R_S$, typical for the evaporated particles, there is already a minimum transverse uncertainty in the image location, $\Delta x > R_S$, that is, the images are not sharper than a particle de Broglie wavelength. Then we get

$$\Delta x^2 > L \lambda_P, \tag{3}$$

which is just the holographic uncertainty at distance L. This uncertainty does not depend on R_S or any property of the hole, only on L, so we identify it as a property of flat spacetime. Formally we may take R_S to vanish and require that black holes of any size have unitary evaporation. If positions in flat spacetime have this transverse indeterminacy, in addition to the Heisenberg uncertainty, then a black hole of any size can leave behind a state with the same size Hilbert space it started with. Since the uncertainty in the distant space does not depend on any property of the hole, it must apply to positions in the spacetime even if there is no hole at all.

Degrees of Freedom of a Massless Field

In a certain sense, holographic indeterminacy is a general property of any frequency-bounded wave field.

Consider a cubic volume of space with a massless scalar field obeying the linear wave equation with reflecting walls. It is conventional to decompose solutions into discrete sinusoidal modes that fit in the box. Given an upper bound on wave frequency, the number of modes is proportional to the 3D volume.

When such a field is quantized, the modes are identified as harmonic oscillators and separately quantized. Each one is identified as a degree of freedom. Thus, the number of degrees of freedom appears to be proportional to volume. Each mode has a number operator and this is one way to decompose the quantum states of the field.

This view is however misleading. Field configurations can also be built from a sum of radiation entering along each face of the cube, with a cutoff in transverse wavenumber corresponding to the maximum frequency. The number of degrees of freedom for propagating waves and particles thus appears to be proportional to surface area, not volume.

The reconciliation of these two descriptions is that the 3D modes are not really independent degrees of freedom. The linear decomposition makes it look that way, and certainly one can build any classical solution by adding linear plane wave mode solutions. But the 3D plane waves are not independent quantum degrees of freedom. A given classical field configuration can be described by many different linear combinations. In the quantum particle description of the states, the localization of a particle in the plane of a wave mode to a small patch on one face of the box implies a transverse momentum uncertainty, and therefore an uncertainty in the wavevector direction, so that the mode is not independent of the others with nearly the same orientation.

This picture describes in general terms the holographic transverse position uncertainty, and nonlocality in the degrees of freedom. A more rigorous derivation showing holographic scaling of total entropy in quantum field theory is given in ref.[10].

WAVE PICTURE OF HOLOGRAPHIC SPACETIME

A physically plausible and informative interpretation of holographic theories uses a wave model of emergent spacetime. The relationship between transverse positions at two times can be described by a quantum wavefunction. In quantum wave language[5], the transverse positions at different times along a null path are conjugate observables, like normal position and momentum in ordinary quantum mechanics, with a commutator $[x_1, x_2] = -ict_{12}\lambda_P$. Their Heisenberg-like uncertainty relation gives the same result for the wavefunction width as a wave optics calculation. The wavefunction can be computed in the same way as transverse mutual complex correlation of field amplitudes for radiation of frequency c/λ_P in standard wave diffraction theory[6]. The width of the mutual complex correlation, the joint wavefunction of transverse position at points separated by ct, increases like $\Delta x \simeq \sqrt{ct\lambda_P}$.

The wave hypothesis developed here is based on the paraxial wave equation, another well studied tool in optics theory. This more general formulation allows a more direct connection with a macroscopic limit of fundamental theories, such as Matrix theory. Once again, the complex phasor amplitude of that theory is taken as a wavefunction for spacetime position. This allows us to write down specific eigenstate wavefunctions, and spatial solutions with specific forms, such as gaussian beams, to compute experimental predictions.

Holographic Hypothesis: Paraxial Wave Equation

A specific way to formulate the holographic hypothesis is to posit that effective spacetime wavefunctions describing macroscopic position states are solutions not of the 3D wave equation, but of the paraxial wave equation.

In the emergent 3D space, the 2D light sheet appears as a wavefront moving at the speed of light. The state is thus naturally described as deviations from the wavefronts of a periodic plane wave. The frequency of the carrier is the fundamental frequency in some given lab frame.

Start with the standard 3D wave equation for a field with a single fixed frequency. In three dimensions, the 3D wave equation for any field component can be written as the modulation of a carrier wave,

$$(\nabla^2 + k^2)E(\vec{x}) = 0. \tag{4}$$

Here $E(\vec{x})$ is a complex phasor representing the amplitude and phase at each point. We use Euclidean coordinates $\vec{x} = x, y, z$ to denote positions in an arbitrary lab rest frame. A sinusoidal time dependence is built in, $E \propto \sin(\omega t)$, where $\omega = ck = 2\pi c/\lambda$. In holographic geometry the carrier is at the Planck frequency.

To derive the paraxial wave equation, we express the field in the form

$$E(x, z) = u(x, z)e^{-ikz}. \tag{5}$$

The field u now describes deviations from a plane wave normal to the z axis. For simplicity, we consider one transverse dimension x and one longitudinal dimension z; identical and independent equations apply to y, z. In laboratory optics applications, z corresponds the direction of a beam, and x to the width of a beam. In our holographic application z corresponds to position in a particular direction that defines the normal axis of a holographic frame, and x to position in a transverse dimension. The wave equation for u becomes

$$\partial^2 u/\partial x^2 + \partial^2 u/\partial z^2 - 2ik\partial u/\partial z = 0. \tag{6}$$

The paraxial approximation is to assume that the second term is negligible compared with the others:

$$\frac{\partial^2 u}{\partial x^2} - 2ik\frac{\partial u}{\partial z} = 0. \tag{7}$$

This equation is proposed as an effective wave equation governing transverse position states of spacetime on macroscopic scales.

It should be emphasized that this phenomenological description is not a fundamental theory. The carrier field is not a dynamical physical field, but a calculational tool. It is constructed to represent the holographic behavior in a lab frame; thus, the wavefunction represents the slowly varying parts of the spatial behavior relative to a Planck frequency plane wave. A true carrier field would not be invariant under boosts to another frame, and neither is this; the wavefunctions are frame-dependent. Similarly, the expansion in paraxial coordinates makes sense if the fundamental theory is built on 2D light sheets, even if the actual wavefronts are not the same in a different lab frame. The theory accurately describes the kind of macroscopic geometrical information that is likely to survive in the classical limit, and therefore is motivated as a proposal for an effective theory.

Relation to Matrix theory

It will be noticed that Eq. (7) is mathematically identical to the one dimensional nonrelativistic Schrödinger wave equation, with z replacing time and $-k$ replacing $m/\hbar$. The interpretation of this equation as a wave equation for spacetime also appears to be a natural consequence in a particular macroscopic interpretation of Matrix theory proposed in ref.[11]. In this interpretation the single transverse coordinate operator $\hat{x}$ refers to the center of mass of a collection of N D0 branes or particles, described as the trace of a fundamental $N \times N$ matrix, one of nine matrices out of which emerge nine spatial dimensions: $\hat{x} = tr\hat{X}$. The emergent 3D system has a maximum frequency equal to the inverse periodicity R of the compactified M dimension, the only scale in the system, assumed in this interpretation to be of order the Planck scale in any lab frame of the emergent spacetime. Modes in the 9 spatial dimensions that emerge from the matrices are not independent on scale R, where the theory is strongly coupled, which indicates that it obeys the holographic bound[4, 11]

The kinematic terms of the Banks et al.[4] Matrix Hamiltonian for the $\hat{X}$ matrix can be written

$$\hat{H} = \frac{R}{2\hbar} tr\hat{\Pi}^2, \tag{8}$$

where $\hat{\Pi}$ denotes the conjugate to $\hat{X}$. This leads to a Schrödinger wave equation resembling Eq. (7) if we make operator identifications similar to those in the standard Schrödinger wave theory, with substitution of the light sheet coordinate $z^+ \equiv (z + ct)/2$ for t in the Hamiltonian operator (since for events on a null trajectory, $z^+ = ct = z$):

$$tr\hat{\Pi}^2 \rightarrow -\hbar^2 \partial^2/\partial x^2, \tag{9}$$

$$\hat{H} \rightarrow i\hbar\partial/\partial z^+, \tag{10}$$

and set $R \rightarrow k^{-1} = \lambda/2\pi$. As in ref. [11], we leave the minus sign in the squared momentum operator, or equivalently, adopt the usual Schrödinger imaginary momentum, $-i\hbar\partial/\partial x$. The wave equation for M theory in one transverse dimension then becomes:

$$\frac{\partial^2 u}{\partial x^2} + \frac{4\pi i}{\lambda}\frac{\partial u}{\partial z^+} = 0. \tag{11}$$

Solutions to Eq. (11) can be expressed as a sum of modes that combine longitudinal and transverse waves:

$$u(x, z^+) = \sum_{k^\perp} A_{k^\perp} \exp -i[k^+ z^+ \pm k^\perp x]. \tag{12}$$

where the wavenumbers of the modes in the two dimensions are related by

$$k^\perp = \sqrt{4\pi k^+/\lambda}. \tag{13}$$

For each mode there is a longitudinal and a transverse wave. For a wavepacket or superposition, describing the position of bodies (the wavefunction for the center of mass of a collection of branes), there is an uncertainty principle in each transverse direction. The conjugate variables in this case are x and $k^\perp$. Their variances $\langle \Delta x^2 \rangle$ and $\langle \Delta k^{\perp 2} \rangle$ in a wavepacket obey uncertainty relations of the usual form,

$$\langle \Delta x^2 \rangle \langle \Delta k^{\perp 2} \rangle \geq 16\pi^2, \tag{14}$$

where the inequality is saturated in the case of gaussian distributions. Using Eq. (13) to convert to the longitudinal wave scale, positions with longitudinal separation on scale $\Delta L^+ \equiv (4\pi/\lambda)(2\pi/\langle\Delta k^{\perp 2}\rangle)$ have a transverse variance

$$\langle \Delta x^2 \rangle > \lambda \Delta L^+ / 2. \tag{15}$$

Note that $\hbar$ has not been assumed to be unity here: it has cancelled out, leaving λ as the only scale in the theory.

This is interpreted as a new kind of uncertainty. A system with a given macroscopic extent has an intrinsic transverse indeterminacy. Since it is formulated here in terms of waves, it does not directly give the precise uncertainty for an apparatus of a given configuration; some other approaches to computing that are suggested below. Still, this line of reasoning connects an effective macroscopic holographic uncertainty to fundamental holographic light sheet theories.

Normally we think of degrees of freedom as almost all residing in independent modes at the microscopic scale. Interferometers are of course exquisitely designed to ignore these and instead measure the envelope wavefunction, the mean or center of mass position of a vast number of particles, on a macroscopic scale. They exclude from the measured signal as many as possible of the internal degrees of freedom that could potentially add more noise. The matrix-theory view of this is that the signal directly encodes the trace of one of the (very large dimensional) fundamental matrices corresponding to the center of mass of the whole body.

Paraxial Representation of Holographic Spacetime

Wave optics language translates straightforwardly into a hypothesis about the quantum states of an emergent, holographic spacetime. The holographic geometry hypothesis is that macroscopic wavefunctions of position transverse to a light sheet obey the paraxial wave equation (Eq. 7), with a fundamental wavelength λ, in terms of the normal coordinate z in any lab frame:

$$\frac{\partial^2 u}{\partial x^2} - \frac{4\pi i}{\lambda}\frac{\partial u}{\partial z} = 0. \tag{16}$$

The z coordinate represents a position along a null trajectory, the emergent direction in the 3D space. In standard Minkowski space coordinates, it is the same as t; however, the wave equation is direction-specific.

The interpretation of this equation is that x represents the center of mass position of a system of particles in one transverse dimension of a flat spacetime. In a particular laboratory frame, x and z are standard Euclidean coordinates. The equation refers to a particular holographic frame with wavefronts normal to z. In this holographic frame, another, independent equation also applies with y replacing x. On the other hand, measurements made with respect to different wavefront orientations do not commute with each other. The photons used to measure the distances between two bodies are in a different holographic frame from the transverse frames that apply to the wavefunction of massive bodies.

This is not an equation of motion of the particles in the standard sense: it refers to the quantum wavefunction of position as limited by the holographic nature of the spacetime. The holographic quantum behavior described by Eq.(16) depends not at all on any properties of the particles, except for their position: all the physics of the field motion and interaction is in addition to this. In the matrix theory argument leading to the paraxial equation, we discarded all the terms describing fermionic activity and noncommutative matrix geometries, and included only the kinematic geometrical terms. The x coordinate is thus interpreted as the center of mass position of all mass and energy in the wavefront.

Gaussian Beam Solutions as Spacetime Wavefunctions

A set of useful solutions of the paraxial wave equation from wave optics is can be applied to describe transverse position states on wavefronts at null separations. They describe beams that fall off transversely with a gaussian profile. These gaussian beams comprise a one-parameter family of solutions, characterized by a longitudinal distance z_R (called the "Rayleigh Range") that physically corresponds to a radius of wavefront curvature at the place where the beam has broadened by a factor of two from its narrowest point. Since the gaussian beams represent the "minimal" transverse uncertainty— they saturate the uncertainty principle— they are a good working model for estimating the level of irreducible, universal holograhic noise in interferometers.

In a given holographic frame, the Gaussian solution to (16) can be expressed as[12, 13]

$$u(x,z) = \frac{w_0}{w(z)} \exp\left[-iz(2\pi/\lambda) - i\phi - x^2\left(\frac{1}{w^2} + \frac{i\pi}{\lambda R}\right)\right] \tag{17}$$

where

$$\phi = \arctan(\lambda z/\pi w_0^2). \tag{18}$$

In optics the quantity R represents the real radius of curvature of the wavefronts. The real part of the wavefunction displays a Gaussian profile in the transverse direction x. The Gaussian width of the beam varies as

$$w(z) = w_0\sqrt{1+(z/z_R)^2} = w_0\sqrt{1+\left(\frac{\lambda z}{\pi w_0^2}\right)^2}, \tag{19}$$

and the radius of curvature

$$R(z) = z\left[1+\left(\frac{\pi w_0^2}{\lambda z}\right)^2\right] \tag{20}$$

The width at the $z = 0$ "waist" for a given solution, corresponding to a flat wavefront, is

$$w_0 = \sqrt{\lambda z_R/\pi}. \tag{21}$$

The width of the beam gradually broadens with propagation due to diffraction. Modes with narrower waists diffract more and broaden more quickly. The minimum transverse width at a distance z occurs for the mode with $z = z_R$. Conversely at a distance z_R , there is a minimum transverse width, $\sqrt{2}w_0 = \sqrt{2\lambda z_R/\pi}$.

A system of spacetime+mass-energy can be put in different states, represented by solutions characterized by w_0 or z_R, by a measurement apparatus. A small transverse width at the waist implies a larger transverse width at large z. For a given z separation between two measurements, there is an optimum state which minimizes the uncertainty in the sum or difference of x for the two measurements. The Gaussian solution is the least uncertain.

In a theory where states are encoded on light sheets with a characteristic or maximum frequency, the transverse width of the position wavefunction displays this minimum diffractive uncertainty. The x observable described by this wavefunction is the position of "everything"— the center of mass of all forms forms of matter and energy on the wavefront.

Relationship of laser and holographic wavefronts

The gaussian-beam picture invites another characterization of holographic uncertainty: at each separation, it is the minimum width of a coherent beam of Planck wavelength radiation. Since the occupation number of Planck wavelength states cannot exceed unity, holographic noise corresponds to the standard quantum limit, at the free spectral range, of an interferometer that uses Planck-wavelength radiation.

The magnitude of the effect in this extreme system can be estimated from momentum perturbation. Suppose we could build an interferometer with a Planck wavelength laser, at maximum power and maximum beamsplitter mass. All elements of such a system are Planck-limited— for example, the optics have at most a Planck mass per Planck area of surface density, $\approx M_P/\lambda_P^2$. For an interferometer of with arm lengths L, the beam waist is $\approx \sqrt{\lambda_P L}$ so the beamsplitter mass is $M_{BS} \approx M_P L/\lambda_P$. In a time L/c, there are $N_\gamma \approx L/\lambda_P$ photons at maximum power, causing a perturbation in beamsplitter velocity $\Delta v_{BS} \approx M_P c\sqrt{N_\gamma}/M_{BS}$. Once again the perturbation beamsplitter position after a time L/c is $\approx \sqrt{\lambda_P L}$.

It is also illuminating to consider the curvature of wavefronts. A wavefront with radius R bends longitudinally by λ over a transverse width $\sqrt{\lambda R}$. Consider a perfectly shaped and measured laser beam wavefront, but assign it a minimum longitudinal width λ_P, that is, a minimum length or maximum frequency in the lab frame. The wavefront position cannot be defined more precisely than this in any experiment. Then the same phase will be measured everywhere in a patch of size $\approx \sqrt{\lambda_P R}$. In the wavefunction interpretation, this is equivalent to saying that the position wavefunction is spread over a patch of this size. If the beam interferes with a similar orthogonal beam at a beamsplitter having this wavefunction, the phase difference cannot be measured with higher precision than this width. (Even though the beamsplitter is at the waist of a beam, so the real radius of curvature diverges, the complex part of the position wavefunction still "knows about" the mode radius and imprints a transverse profile on the outcome of a measurement.) In an optical cavity of any arm length, the holographic transverse uncertainty is smaller than the optical beam waist by a factor $\approx \sqrt{\lambda_P/\lambda_{opt}}$.

It is also useful to reflect again on the black hole thought experiment. At a distance $< R_S^2/\lambda_P$ from the hole, the transverse uncertainty of evaporated particles is dominated by the Heisenberg uncertainty, and the gravitational curvature of wavefronts is bigger, that is, with smaller radius than the holographic curvature radius. At larger distance, the holographic uncertainty dominates and is independent of the (at this distance very small) gravitational effect of the hole.

STATISTICS OF HOLOGRAPHIC NOISE IN SIGNALS

Holographic uncertainty (in analogy to Heisenberg uncertainty) can be defined as the minimum of the product of the widths of transverse wavefunctions u at some separation L. The value of the difference of the positions is indeterminate, leading to holographic indeterminacy in an instrument, such as an interferometer, that measures such a difference. Holographic noise comes about because the indeterminacy leads to a random variation in the measured position as a function of time.

Setting λ from Black Hole Physics

The wave theory is normalized by matching degrees of freedom to gravitational physics. We require the theory to agree with the entropy per transverse lightsheet area from black hole thermodynamics,

$$S_H/A = (4\lambda_P^2)^{-1}, \tag{22}$$

where Boltzmann's k is set equal to unity.

This entropy corresponds to one degree of freedom per $2\lambda_P$ in each transverse direction. Standard quantization for a confined scalar particle gives one degree of freedom per λ for each direction. These agree if the effective fundamental wavelength, for macroscopic purposes, is twice the standard definition of the Planck length:

$$\lambda_0 \equiv 2\pi/k_0 \equiv ct_0 = 2\lambda_P \equiv 2ct_P. \tag{23}$$

Henceforth we will normalize to this value for predictions of observable effects.

This may be an exactly correct value for all practical purposes, since it invokes new physics only via gravitational entropy, which is well calibrated with ordinary entropy using the theory of black hole evaporation. However, this derivation falls short of a rigorous proof, since it does not offer a detailed characterization of the actual degrees of freedom. A better understanding of the fundamental degrees of freedom, and how they relate to gravity, is one goal of an experimental program.

Autocorrelation of Displacement

Suppose we have a way of measuring transverse position as a function of time along a light sheet trajectory. In an appropriate setting we can interpret $u(x, z)$ as a quantum wavefunction and use it to compute the time correlation of the measurements.

We wish to compute the statistical properties of a signal, a scalar phase as a function of time. Suppose that the effect of holographic noise mimics a classical motion of the beamsplitter as described above. Denote by $X(t)$ the difference in position of the beamsplitter along the two arm directions at time t in a lab frame. The time correlation of the classical scalar X is defined as the limiting average,

$$\Xi(\tau) = \lim_{T\to\infty} (2T)^{-1} \int_{-T}^{T} dt X(t)X(t+\tau) \tag{24}$$

In a particular interferometer optical configuration (depending on signal recycling, folded arms, Fabry-Perot arm cavities, etc.), $\Xi(\tau)$ determines the statistics of the noise in the signal.

The two measurement events are on wavefronts separated by $c\tau$. We model the wavefunction as a gaussian beam mode where the radius $z_R = c\tau/2$. The correlation (Eq. 24) at lag $\tau = 0$ is given by the mean square displacement determined by the wavefunction (Eq. 17) with $z_R = c\tau/2$, with an extra factor of 2 because we add the variance from two events:

$$\Xi(\tau = 0) = 2 \int dx x^2 u^*(x, z = z_R = c\tau/2)u(x, z = z_R = c\tau/2). \tag{25}$$

The standard deviation of each gaussian u is $\sigma = w/\sqrt{2}$; for their product, $\sigma = w/2$. Twice the mean square then is given by $\Xi(\tau) = 2w^2(z = z_R)/4 = w_0^2 = z_R\lambda/\pi = c\tau\lambda/2\pi$.

In the case of an in-line interferometer, where one arm is bent back away from the other, so the light in the two arms travels in opposite directions, there would be an added factor of $\sqrt{2}$ because the effective motion of the beamsplitter adds to one while it subtracts from the other. There may be other factors of order unity arising if there is a different wave solution from the Gaussian-beam model.

In the classical limit, the transverse motion mimics a random walk. For each Planck length of longitudinal propagation, there is a transverse step of about a Planck length, in a random direction, along each transverse direction. In an interferometer of finite size, there is a limit to the random walk. Let L denote the length of the arms, so that $2L$ is the round trip travel time. As illustrated by the wave solutions above, over longer times, the signal does not show the holographic noise, since the whole apparatus "moves" together. The random walk for the position observable therefore has a bound imposed at time $2L/c$. The time autocorrelation of classical position is then

$$\Xi(\tau) = (ct_0/2\pi)[2L - c\tau], \qquad \tau < 2L/c. \tag{26}$$

The standard deviation saturates at the value for $\tau = 2L/c$, so

$$\Xi(\tau) = 0, \qquad \tau > 2L/c. \tag{27}$$

These formulas do not capture the correct behavior at very small $c\tau$, less than the beam diameter, say. However, for practical purposes Eqs. (26) and (27) are a description of the classical behavior. Time-domain sampling of the signal is predicted to show this correlation.

The behavior can also be described in the frequency domain. The power spectrum $\Phi(f)$ is given by the Wiener theorem,

$$\Phi(f) = 2\int_0^\infty d\tau \Xi(\tau)\cos(\tau\omega), \tag{28}$$

where $\omega = 2\pi f$.[14] Integration of this formula using Eqs.(26) and (27) gives an exact prediction for the spectrum.

The low frequency limit ($f << c/2L$) gives a flat spectrum independent of f:

$$\Phi(f) \approx 2t_0L^2/\pi = 4t_PL^2/\pi, \qquad f << c/2L. \tag{29}$$

The power spectrum decreases at higher frequencies; in the high frequency limit it is independent of L,

$$\Phi(f) \propto \frac{c^2t_P}{f^2}, \tag{30}$$

as one would expect for a universal noise. The apparatus size— the distance over which the sampling occurs— acts as a high-pass filter; fluctuations from longer longitudinal modes do not enter into the signal.

Apparent Gravitational Wave Spectrum

A model of an apparatus using the beamsplitter position correlation function (Eqs. 26, 27) as a description of effective classical motion allows an exact prediction of the signal statistics at all frequencies. Current results are generally quoted in terms of equivalent gravitational wave strain, which requires a consideration of the gravitational wave transfer function of an apparatus.

In the low frequency limit (Eq. 29), the effective holographic beamsplitter displacement noise in a folded Michelson interferometer creates the same noise spectrum as an amplitude spectral density of gravitational waves,

$$h(f) = \mathcal{N}^{-1}\sqrt{\Phi/L^2} = \mathcal{N}^{-1}2\sqrt{t_P/\pi} = \mathcal{N}^{-1}2.6\times10^{-22}/\sqrt{\text{Hz}}, \tag{31}$$

where $\mathcal{N}$ is the average number of photon round trips in the interferometer arms.

The reason for the added factor of $\mathcal{N}^{-1}$ is that folded arms (as in GEO600), or Fabry-Perot cavities (as in LIGO) with finesse $\approx \pi\mathcal{N}$, amplify the signal response to a gravitational wave strain, but not to holographic noise. For a given physical displacement of the beamsplitter and inboard folding mirrors, the measured phase displacement corresponds to a gravitational-wave strain proportional to $\mathcal{N}^{-1}$ at frequencies below $\approx c/2L\mathcal{N}$. The folding effectively lengthens the arms for gravitational wave detection, but does not amplify the holographic noise in the signal. The effect of

the displacement noise on the signal (both from the beamsplitter, and from the inboard mirrors in the case of folded configurations) just depends on the actual size of the arms. (Another view of this effect is to note that a low frequency strain wave causes displacements which are always opposite in the two arms, and therefore accumulate additional effect on the dark port signal.)

In GEO600, with $\mathcal{N} = 2$, the estimate in Eq.(31) predicts a new noise source, $h = \sqrt{t_P/\pi} = 1.3 \times 10^{-22}/\sqrt{\text{Hz}}$, at all measured frequencies. This holographic noise spectrum approximately agrees with currently unexplained "mystery noise" in GEO600, above about 500Hz.

In ref. [6] a similar result was derived, by a calculation based on a wave-optics model similar to that presented here. In that paper however it was erroneously claimed that in a power recycling cavity the predicted slope changes at very low frequencies, below an inverse power-recycling time. In fact the apparent gravitational wave spectrum corresponding to a bounded random walk of the beamsplitter is just flat as in Eq. (31). In addition, the numerical factor in ref. [6] was different, $h = \sqrt{t_P/2}$ instead of $h = \sqrt{t_P/\pi}$, so the predicted noise is now less, by about 20%. The current calculation takes into account the detailed profile of the gaussian mode solution, Eq. (21), which is likely to be a more physically realistic model of instrument/spacetime wavefunction, and should be taken as a more reliable calculation than the earlier one of the actual minimum level of noise. (This prediction, however, should still not be considered definitive, since the description of the apparatus is still a hybrid of classical and wave models.) Low frequency excess noise in GEO600 is still unexplained, but the holographic prediction still approximately fits the unexplained noise above about 500 Hz. Indeed if it is real, holographic noise is currently the dominant noise source in GEO600 at its most sensitive frequency— about half of the measured noise power.

GEO600 is more sensitive than LIGO to beamsplitter displacement, even if it is less sensitive to gravitational waves. The holographic noise predicted in LIGO is below current limits by a significant factor due to its Fabry-Perot arm cavities, which have $\mathcal{N} \approx 10^2$. Without the factor of $\mathcal{N}$— that is, if the noise lacked the specific transverse shear character of holographic noise— current LIGO limits rule out excess noise with this amplitude. For this reason, LIGO data already rule out models predicting Planck-amplitude noise in the metric, which has a strain character[7–9]. Advanced LIGO may become holographic-noise-limited at its most sensitive frequencies.

At frequencies above $\approx c/2L$, the apparent noise spectrum in an unfolded system turns over to $h(f) \propto (c/fL)\sqrt{t_P}$. For a folded system, the amplification of the effect of gravitational waves on the signal decreases above a frequency $\approx c/2L\mathcal{N}$, since there are fewer roundtrips per wave cycle. Thus the equivalent gravitational wave spectrum actually rises from there up to a frequency $\approx c/2L$, above which it is about the same as an unfolded system.

Cross Correlation of Two Instruments

An experiment designed to provide convincing evidence for or against the holographic hypothesis could include more than one interferometer. Two separate interferometers, with no physical connection aside from inhabiting the same holographic spacetime, should nevertheless show correlated holographic noise. This feature can be used to design an experiment with purely holographic signatures in the signal.

Consider two aligned interferometers, both with arms of length L parallel to the x and y axes. Suppose one is placed vertically above the other, with vertical displacement L_z. If $L_z << L$, the holographic position displacements of the two beamsplitters are almost the same.

To see that this coherence must occur, consider the holographic frame with wavefronts aligned normal to the z axis, that is, parallel to the xy plane containing the two arms. The positions of the two instruments at null separation (times differing by L_z/c in the lab frame) are described by data on the same holographic wavefront. The uncorrelated x, y holographic displacement between the two at any time along each axis is then given by the transverse uncertainty in this frame, which is only $\Delta x = \Delta y = \sqrt{ct_0 L_z}$; the rest of the apparent motion must be correlated. Therefore, for small $L_z << L$, the cross correlation must be nearly perfect; the spacetime wavefunctions for the differences of x and y between the two systems are very narrow compared to the total wavefunction width corresponding to $\sqrt{ct_0 L}$. This follows as long as the two transverse degrees of freedom are independent in any holographic frame, so it is a robust prediction.

If L_z is not negligible, the prediction from this description is not as well controlled, but we can make guesses at the approximate behavior. For significant L_z we guess at a cross correlation roughly of the form

$$\Xi_\times(\tau) = 0 \qquad c\tau < 2L_z \tag{32}$$

$$= ct_0(2L - c\tau - 2L_z)/2\pi \qquad 2L_z < c\tau < 2L - 2L_z \tag{33}$$

$$= 0 \qquad c\tau > 2L - 2L_z. \tag{34}$$

Thus if the vertical displacement is small compared to L, the cross correlation is almost the same as the autocorrelation of a single machine. For vertical displacement greater than L, the cross correlation disappears, as expected from the indeterminacy predicted for large separations in the z-normal (vertical) frame. Although the paraxial approximation predicted a perfect correlation with z displacement, for large vertical displacement the paraxial description is not accurate (for example, higher order effects of wavefront curvature relative to plane waves cannot be neglected, so light cones no longer map onto wavefronts) so the decoherence is not surprising. The first generation machine to test the holographic hypothesis should be built with a small $L_z << L$ since the cross correlation is well understood in this situation.

The holographic framework also allows an informed guess for the cross correlation in situations with displacements along the x and y arms. Let L_x and L_y denote displacements between the two interferometers along those directions. Denote the larger in-plane displacement by

$$L_{max} = \max[L_x, L_y]. \tag{35}$$

The correlated part is determined by the transverse motion accumulated over the in-common path— the length over which laser light wavefronts are travelling at the same time, in the same direction, in both arms of both interferometers. For zero L_z, the integrated correlation is proportional to $L - L_{max}$. Allowing in addition for z displacement, we define a characteristic total effective displacement

$$L'_{max} = L_{max} + L_z, \tag{36}$$

so that $L - L'_{max}$ is the effective length creating cross-correlated displacements.

Then we guess at a cross correlation of the form

$$\begin{aligned} \Xi_\times(\tau) &= 0 \qquad\qquad c\tau < 2L'_{max} && (37)\\ &= ct_0(2L - c\tau - 2L'_{max})/2\pi \qquad 2L'_{max} < c\tau < 2L - 2L'_{max} && (38)\\ &= 0 \qquad c\tau > 2L - 2L'_{max} && (39) \end{aligned}$$

The cross correlation gradually disappears as the interferometers are separated in any direction. For zero vertical displacement, the cross correlation occurs only at times when aligned laser beam wavefronts are traveling in both arms of both interferometers at the same time. If the in-plane displacement exceeds the arm length in either direction, or if the vertical displacement exceeds the in-common length $L - L_{max}$, the correlation disappears.

These formulas probably describe the decorrelation accurately for small displacements, but we have not proved that they apply for L'_{max} comparable to L. They apply also to two aligned and displaced in-line interferometers, where L_{max} is taken to denote the in-line displacement and L_z corresponds to the displacement transverse to the interferometer axis. The formulae satisfy the criterion that the reflection events that collapse the wavefunction occur at correlated locations only when they lie within a classical causal light cone.

The frequency spectrum of the cross correlation signal is given as above using the Wiener formula. For $L'_{max} > 0$, the noise power is reduced at all frequencies. The low frequency limit becomes

$$\Phi_\times(f) \approx 4t_P L^2[1 - (L'_{max}/L)]/\pi, \qquad f << c/2L. \tag{40}$$

EXPERIMENTAL PROGRAM

It appears that an experiment that reaches this level of position sensitivity is guaranteed to provide informative results about physics at the Planck scale. That is, a null result excluding cross correlated noise in two systems, in contradiction to holographic theories, will imply that at least one of the two features outlined above (Planck frequency bound, or holographic information bound) does not hold. A positive result of course opens up a whole field of followup experiments that will illuminate the way that Planck-scale quantum physics maps onto the macroscopic, quasi-classical world.

A new experiment[15] is therefore motivated to test the holographic hypothesis presented here. The most distinctive prediction is the correlation between two close but not connected interferometers. For two aligned interferometers with a fractionally small displacement, a cross correlation in the holographic noise displacement is robustly predicted on general theoretical grounds. The two interferometers can be in separate cavities and Faraday isolated to exclude other sources of in-common noise in the relevant band. The dominant noise source, photon shot noise, is uncorrelated between the two and averages in time to zero, while the holographic noise is in common and averages to a definite

known value. This allows an experiment on a much smaller scale (and higher frequencies) than the interferometric gravitational wave detectors, even though the photon shot noise dominates by a large factor at high frequencies.

Consider a pair of adjacent and aligned power-recycled interferometers. The time required for the cross correlation from holographic noise to equal the photon shot noise at frequency $c/2L$ is[15]

$$t_{\gamma\times} \approx \left[\frac{\lambda_{opt}^2}{L^3(2\pi)^4}\right]\left[\frac{c^3}{\lambda_P^2}\right]\left[\frac{h_P}{P_{opt}}\right]^2 \tag{41}$$

where λ_{opt} and P_{opt} refer to the wavelength and power of the laser cavity, h_P is Planck's constant, and L is the arm length. This becomes

$$t_{\gamma\times} \approx 375 \text{ s } (P_{opt}/1000\text{w})^{-2}(L/40\text{m})^{-3}. \tag{42}$$

Thus there is a trade between system size and laser power. The optimum appears to be a system with arms some tens of meters in length; for shorter arms, the large required power in the cavity and smaller waist size cause significant heating in the optics. For a system with 40m arms, the characteristic frequency is $c/2L = 3.5$ MHz. With 1000 watt cavities, the correlated power matches the photon shot noise power after about $t_{\gamma\times} \approx 5$ minutes. The significance of a detection after time t is about $(t/t_{\gamma\times})^{1/2}$ standard deviations. Modern experimental techniques can sample and correlate data rapidly enough to study both time and frequency domain correlations in this regime.

For small fractional displacement between instruments, the predictions here are motivated on general grounds, but they become less reliable as the displacement approaches the apparatus size. If two close interferometers yield a positive result, a followup experimental program with different experimental geometries would inform this aspect of the theory.

I am grateful for discussions and correspondence with many colleagues, including particularly A. Chou, H. Grote, S. Hild, H. Lück, G. Müller, B. Schutz, S. Waldman, R. Weiss, S. Whitcomb, G. Woan, and other participants in the Hannover workshop on holographic noise. This work was supported by the Department of Energy.

[1] G. 't Hooft, "Dimensional reduction in quantum gravity," in "Conference on Particle and Condensed Matter Physics (Salamfest)", edited by A. Ali, J. Ellis, and S. Randjbar-Daemi (World Scientific, Singapore, 1993), arXiv:gr-qc/9310026.
[2] L. Susskind, "The World As A Hologram," J. Math. Phys. **36**, 6377 (1995)
[3] R. Bousso, "The holographic principle," Rev. Mod. Phys. **74**, 825 (2002)
[4] T. Banks, W. Fischler, S. H. Shenker and L. Susskind, "M theory as a matrix model: A conjecture," Phys. Rev. D **55**, 5112 (1997)
[5] C. J. Hogan, "Measurement of Quantum Fluctuations in Geometry," Phys. Rev. D 77, 104031 (2008), arXiv:0712.3419
[6] C. J. Hogan, "Indeterminacy of Quantum Geometry," Phys Rev D.78.087501 (2008), arXiv:0806.0665
[7] G. Amelino-Camelia, "Gravity-wave interferometers as probes of a low-energy effective quantum gravity," Phys. Rev. D **62**, 024015 (2000)
[8] G. Amelino-Camelia, "A phenomenological description of quantum-gravity-induced space-time noise," Nature **410**, 1065 (2001)
[9] Y. J. Ng, "Quantum foam and quantum gravity phenomenology," Lect. Notes Phys. **669**, 321 (2005) [arXiv:gr-qc/0405078].
[10] M. Srednicki, "Entropy and area," Phys. Rev. Lett. **71**, 666 (1993)
[11] C. J. Hogan and M. G. Jackson, "Holographic Geometry and Noise in Matrix Theory," Phys. Rev. D. in press, arXiv:0812.1285 [hep-th].
[12] H. Kogelnik, T., Li, "Laser Beams and Resonators", Appl. Opt. 5, 1550 (1966)
[13] A. E. Siegman, *Lasers*, Sausalito: University Science Books (1986).
[14] J. B. Camp, N.J. Cornish, "Gravitational Wave Astronomy", Ann. Rev. Nuc. Part. Sci. 54, 525 (2004)
[15] R. Weiss, "Concept for an interferometric test of Hogan's quantum geometry hypothesis", 2/10/2009.